

## **The NEURON Simulation Environment**

M.L. Hines<sup>1,3</sup> and N.T. Carnevale<sup>2,3</sup>

Departments of <sup>1</sup>Computer Science and <sup>2</sup>Psychology

and <sup>3</sup>Neuroengineering and Neuroscience Center

Yale University

michael.hines@yale.edu

ted.carnevale@yale.edu

To appear in *Neural Computation*, Volume 9, Number 6 (August 15, 1997),  
copyright © 1997 by the Massachusetts Institute of Technology, all rights reserved.

## 1. INTRODUCTION

NEURON (Hines 1984; 1989; 1993; 1994) provides a powerful and flexible environment for implementing biologically realistic models of electrical and chemical signaling in neurons and networks of neurons. This article describes the concepts and strategies that have guided the design and implementation of this simulator, with emphasis on those features that are particularly relevant to its most efficient use.

### 1.1 The problem domain

Information processing in the brain results from the spread and interaction of electrical and chemical signals within and among neurons. This involves nonlinear mechanisms that span a wide range of spatial and temporal scales (Carnevale and Rosenthal 1992) and are constrained to operate within the intricate anatomy of neurons and their interconnections. Consequently the equations that describe brain mechanisms generally do not have analytical solutions, and intuition is not a reliable guide to understanding the working of the cells and circuits of the brain. Furthermore, these nonlinearities and spatiotemporal complexities are quite unlike those that are encountered in most nonbiological systems, so the utility of many quantitative and qualitative modeling tools that were developed without taking these features into consideration is severely limited.

NEURON is designed to address these problems by enabling both the convenient creation of biologically realistic quantitative models of brain mechanisms and the efficient simulation of the operation of these mechanisms. In this context the term “biological realism” does not mean “infinitely detailed.” Instead it means that the choice of which details to include in the model and which to omit are at the discretion of the investigator who constructs the model, and not forced by the simulation program.

To the experimentalist NEURON offers a tool for cross-validating data, estimating experimentally inaccessible parameters, and deciding whether known facts account for experimental observations. To the theoretician it is a means for testing hypotheses and determining the smallest subset of anatomical and biophysical properties that is necessary and sufficient to account for particular phenomena. To the student in a laboratory course it provides a vehicle for illustrating and exploring the operation of brain mechanisms in a simplified form that is more robust than the typical “wet lab” experiment. For experimentalist, theoretician, and student alike, a powerful simulation tool such as NEURON can be an indispensable aid to developing the insight and intuition that is needed if one is to discover the order hidden within the intricacy of biological phenomena, the order that transcends the complexity of accident and evolution.

### 1.2 Experimental advances and quantitative modeling

Experimental advances drive and support quantitative modeling. Over the past two decades the field of neuroscience has seen striking developments in experimental techniques that include

- high-quality electrical recording from neurons *in vitro* and *in vivo* using patch clamp
- multiple impalements of visually identified cells
- simultaneous intracellular recording from paired pre- and postsynaptic neurons
- simultaneous measurement of electrical and chemical signals
- multisite electrical and optical recording
- quantitative analysis of anatomical and biophysical properties from the same neuron
- photolesioning of cells

- photorelease of caged compounds for spatially precise chemical stimulation
- new drugs such as channel blockers and receptor agonists and antagonists
- genetic engineering of ion channels and receptors
- analysis of mRNA and biophysical properties from the same neuron
- “knockout” mutations

These and other advances are responsible for impressive progress in the definition of the molecular biology and biophysics of receptors and channels, the construction of libraries of identified neurons and neuronal classes that have been characterized anatomically, pharmacologically, and biophysically, and the analysis of neuronal circuits involved in perception, learning, and sensorimotor integration.

The result is a data avalanche that catalyzes the formulation of new hypotheses of brain function, while at the same time serving as the empirical basis for the biologically realistic quantitative models that must be used to test these hypotheses. Some examples from the large list of topics that have been investigated through the use of such models include

- the cellular mechanisms that generate and regulate chemical and electrical signals (Destexhe et al. 1996; Jaffe et al. 1994)
- drug effects on neuronal function (Lytton and Sejnowski 1992)
- presynaptic (Lindgren and Moore 1989) and postsynaptic (Destexhe and Sejnowski 1995; Traynelis et al. 1993) mechanisms underlying communication between neurons
- integration of synaptic inputs (Bernander et al. 1991; Cauller and Connors 1992)
- action potential initiation and conduction (Häusser et al. 1995; Hines and Shragar 1991; Mainen et al. 1995)
- cellular mechanisms of learning (Brown et al. 1992; Tsai et al. 1994a)
- cellular oscillations (Destexhe et al. 1993a; Lytton et al. 1996)
- thalamic networks (Destexhe et al. 1993b; Destexhe et al. 1994)
- neural information encoding (Hsu et al. 1993; Mainen and Sejnowski 1995; Softky 1994)

## 2. OVERVIEW OF NEURON

NEURON is intended to be a flexible framework for handling problems in which membrane properties are spatially inhomogeneous and where membrane currents are complex. Since it was designed specifically to simulate the equations that describe nerve cells, NEURON has three important advantages over general purpose simulation programs. First, the user is not required to translate the problem into another domain, but instead is able to deal directly with concepts that are familiar at the neuroscience level. Second, NEURON contains functions that are tailored specifically for controlling the simulation and graphing the results of real neurophysiological problems. Third, its computational engine is particularly efficient because of the use of special methods and tricks that take advantage of the structure of nerve equations (Hines 1984; Mascagni 1989).

However, the general domain of nerve simulation is still too large for any single program to deal optimally with every problem. In practice, each program has its origin in a focused attempt to solve a restricted class of problems. Both speed of simulation and the ability of the user to maintain conceptual control degrade when any program is applied to problems outside the class for which it is best suited.

NEURON is computationally most efficient for problems that range from parts of single cells to small numbers of cells in which cable properties play a crucial role. In terms of conceptual control, it is best suited to tree-shaped structures in which the membrane channel parameters are approximated by piecewise

linear functions of position. Two classes of problems for which it is particularly useful are those in which it is important to calculate ionic concentrations, and those where one needs to compute the extracellular potential just next to the nerve membrane. It is especially capable for investigating new kinds of membrane channels since they are described in a high level language (NMODL (Moore and Hines 1996)) which allows the expression of models in terms of kinetic schemes or sets of simultaneous differential and algebraic equations. To maintain efficiency, user defined mechanisms in NMODL are automatically translated into C, compiled, and linked into the rest of NEURON.

The flexibility of NEURON comes from a built-in object oriented interpreter which is used to define the morphology and membrane properties of neurons, control the simulation, and establish the appearance of a graphical interface. The default graphical interface is suitable for exploratory simulations involving the setting of parameters, control of voltage and current stimuli, and graphing variables as a function of time and position.

Simulation speed is excellent since membrane voltage is computed by an implicit integration method optimized for branched structures (Hines 1984). The performance of NEURON degrades very slowly with increased complexity of morphology and membrane mechanisms, and it has been applied to very large network models ( $10^4$  cells with 6 compartments each, total of  $10^6$  synapses in the net [T. Sejnowski, personal communication]).

### 3. MATHEMATICAL BASIS

Strategies for numerical solution of the equations that describe chemical and electrical signaling in neurons have been discussed in many places. Elsewhere we have briefly presented an intuitive rationale for the most commonly used methods (Hines and Carnevale 1995). Here we start from this base and proceed to address those aspects which are most pertinent to the design and application of NEURON.

#### 3.1 The cable equation

The application of cable theory to the study of electrical signaling in neurons has a long history, which is briefly summarized elsewhere (Rall 1989). The basic computational task is to numerically solve the cable equation

$$\frac{\partial V}{\partial t} + I(V, t) = \frac{\partial^2 V}{\partial x^2} \quad (1)$$

which describes the relationship between current and voltage in a one-dimensional cable. The branched architecture typical of most neurons is incorporated by combining equations of this form with appropriate boundary conditions.

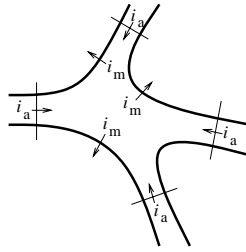


Figure 3.1. The net current entering a region must equal zero.

Spatial discretization of this partial differential equation is equivalent to reducing the spatially distributed neuron to a set of connected compartments. The earliest example of a multicompartmental approach to the analysis of dendritic electrotonus was provided by Rall (1964).

Spatial discretization produces a family of ordinary differential equations of the form

$$c_j \frac{dv_j}{dt} + i_{ionj} = \sum_k \frac{v_k - v_j}{r_{jk}} \quad (2)$$

Equation 2 is a statement of Kirchhoff's current law, which asserts that net transmembrane current leaving the  $j$ th compartment must equal the sum of axial currents entering this compartment from all sources (Fig. 3.1). The left hand side of Eq. 2 is the total membrane current, which is the sum of capacitive and ionic components. The capacitive component is  $c_j dv_j/dt$ , where  $c_j$  is the membrane capacitance of the compartment. The ionic component  $i_{ionj}$  includes all currents through ionic channel conductances. The right hand side of Eq. 2 is the sum of axial currents that enter this compartment from its adjacent neighbors. Currents injected through a microelectrode would be added to the right hand side. The sign conventions for current are: outward transmembrane current is positive; axial current flow into a region is positive; positive injected current drives  $v_j$  in a positive direction.

Equation 2 involves two approximations. First, axial current is specified in terms of the voltage drop between the centers of adjacent compartments. The second approximation is that spatially varying membrane current is represented by its value at the center of each compartment. This is much less drastic than the often heard statement that a compartment is assumed to be "isopotential." It is far better to picture the approximation in terms of voltage varying linearly between the centers of adjacent compartments. Indeed, the linear variation in voltage is implicit in the usual description of a cable in terms of discrete electrical equivalent circuits.

If the compartments are of equal size, it is easy to use Taylor's series to show that both of these approximations have errors proportional to the square of compartment length. Thus replacing the second partial derivative by its central difference approximation introduces errors proportional to  $\Delta x^2$ , and doubling the number of compartments reduces the error by a factor of four.

It is often not convenient for the size of all compartments to be equal. Unequal compartment size might be expected to yield simulations that are only first order accurate. However, comparison of simulations in which unequal compartments are halved or quartered in size generally reveals a second-order reduction of error. A rough rule of thumb is that simulation error is proportional to the square of the size of the largest compartment.

The first of two special cases of Eq. 2 that we wish to discuss allows us to recover the usual parabolic differential form of the cable equation. Consider the interior of an unbranched cable with constant

diameter. The axial current consists of two terms involving compartments with the natural indices  $j-1$  and  $j+1$ , i.e.

$$c_j \frac{dv_j}{dt} + i_{ion_j} = \frac{v_{j-1} - v_j}{r_{j-1,j}} + \frac{v_{j+1} - v_j}{r_{j,j+1}}$$

If the compartments have the same length  $\Delta x$  and diameter  $d$ , then the capacitance of a compartment is  $C_m \pi d \Delta x$  and the axial resistance is  $R_a \Delta x / \pi (d/2)^2$ .  $C_m$  is called the specific capacitance of the membrane, which is generally taken to be  $1 \mu\text{f} / \text{cm}^2$ .  $R_a$  is the axial resistivity, which has different reported values for different cell classes (e.g.  $35.4 \Omega \text{ cm}$  for squid axon). Eq. 2 then becomes

$$C_m \frac{dv_j}{dt} + i_j = \frac{d}{4R_a} \frac{v_{j+1} - 2v_j + v_{j-1}}{\Delta x^2}$$

where we have replaced the total ionic current  $i_{ion_j}$  with the current density  $i_j$ . The right hand term, as  $\Delta x \rightarrow 0$ , is just  $\partial^2 V / \partial x^2$  at the location of the now infinitesimal compartment  $j$ .

The second special case of Eq. 2 allows us to recover the boundary condition. This is an important exercise since naive discretizations at the ends of the cable have destroyed the second order accuracy of many simulations. Nerve boundary conditions are that no axial current flows at the end of the cable, i.e. the end is sealed. This is implicit in Eq. 2, where the right hand side consists only of the single term  $(v_{j-1} - v_j) / r_{j-1,j}$  when compartment  $j$  lies at the end of an unbranched cable.

### 3.2 Spatial discretization in a biological context: sections and segments

Every nerve simulation program solves for the longitudinal spread of voltage and current by approximating the cable equation as a series of compartments connected by resistors (Fig. 3.4 and Eq. 2). The sum of all the compartment areas is the total membrane area of the whole nerve. Unfortunately, it is usually not clear at the outset how many compartments should be used. Both the accuracy of the approximation and the computation time increase as the number of compartments used to represent the cable increases. When the cable is “short,” a single compartment can be made to adequately represent the entire cable. For long cables or highly branched structures, it may be necessary to use a large number of compartments.

This raises the question of how best to manage all the parameters that exist within these compartments. Consider membrane capacitance, which has a different value in each compartment. Rather than specify the capacitance of each compartment individually, it is better to deal in terms of a single specific membrane capacitance which is constant over the entire cell and have the program compute the values of the individual capacitances from the areas of the compartments. Other parameters such as diameter or channel density may vary widely over short distances, so the graininess of their representation may have little to do with numerically adequate compartmentalization.

Although NEURON is a compartmental modeling program, the specification of biological properties (neuron shape and physiology) has been separated from the numerical issue of compartment size. What makes this possible is the notion of a **section**, which is a continuous length of unbranched cable. Although each section is ultimately discretized into compartments, values that can vary with position along the length

of a section are specified in terms of a continuous parameter that ranges from 0 to 1 (normalized distance). In this way, section properties are discussed without regard to the number of segments used to represent it. This makes it easy to trade off between accuracy and speed, and enables convenient verification of the numerical correctness of simulations.

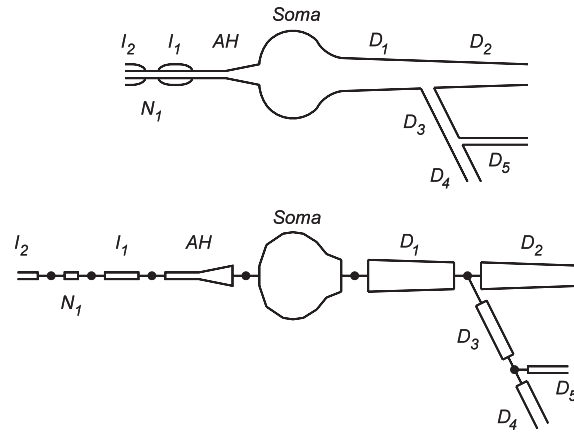


Figure 3.2. Top: cartoon of a neuron indicating the approximate boundaries between biologically significant structures.. The left hand side of the cell body (*Soma*) is attached to an axon hillock (*AH*) that drives a myelinated axon (myelinated internodes  $I_i$  alternating with nodes of Ranvier  $N_i$ ). From the right hand side of the cell body originates a branched dendritic tree ( $D_i$ ). Bottom: how sections would be employed in a NEURON model to represent these structures.

Sections are connected together to form any kind of branched tree structure. Fig. 3.2 illustrates how sections are used to represent biologically significant anatomical features. The top of this figure is a cartoon of a neuron with a soma that gives rise to a branched dendritic tree and an axon hillock connected to a myelinated axon. Each biologically significant component of this cell has its counterpart in one of the sections of the NEURON model, as shown in the bottom of Fig. 3.2: the cell body (*Soma*), axon hillock (*AH*), myelinated internodes ( $I_i$ ), nodes of Ranvier ( $N_i$ ), and dendrites ( $D_i$ ). Sections allow this kind of functional/anatomical parcellation of the cell to remain foremost in the mind of the person who constructs and uses a NEURON model.

To accommodate requirements for numerical accuracy, NEURON represents each section by one or more **segments** of equal length (Figs. 3.3 and 3.4). The number of segments is specified by the parameter **nseg**, which can have a different value for each section.

At the center of each segment is a **node**, the location where the internal voltage of the segment is defined. The transmembrane currents over the entire surface area of a segment are associated with its node. The nodes of adjacent segments are connected by resistors.

It is crucial to realize that the location of the second order correct voltage is not at the edge of a segment but rather at its *center*, i.e. at its node. This is the discretization method employed by NEURON. To allow branching and injection of current at the precise ends of a section while maintaining second order correctness, extra voltage nodes that represent compartments with 0 area are defined at the section ends. It is possible to achieve second order accuracy with sections whose end nodes have nonzero area compartments. However, the areas of these terminal compartments would have to be exactly half that of the internal compartments, and extra complexity would be imposed on administration of channel density at branch points.

Based on the position of the nodes, NEURON calculates the values of internal model parameters such as the average diameter, axial resistance, and compartment area that are assigned to each segment.

Figs. 3.3 and 3.4 show how an unbranched portion of a neuron, called a neurite (Fig. 3.3A), is represented by a section with one or more segments. Morphometric analysis generates a series of diameter measurements whose centers lie on the midline of the neurite (thin axial line in Fig. 3.3B). These measurements and the path lengths between their centers are the dimensions of the section, which can be regarded as a chain of truncated cones or frusta (Fig. 3.3C).

Distance along the length of a section is discussed in terms of the normalized position parameter  $x$ . That is, one end of the section corresponds to  $x = 0$  and the other end to  $x = 1$ . In Fig. 3.3C these locations are depicted as being on the left and right hand ends of the section. The locations of the nodes and the boundaries between segments are conveniently specified in terms of this normalized position parameter. In general, a section has `nseg` segments that are demarcated by evenly spaced boundaries at intervals of  $1 / \text{nseg}$ . The nodes at the centers of these segments are located at  $x = (2i - 1) / 2 \text{nseg}$  where  $i$  is an integer in the range  $[1, \text{nseg}]$ . As we shall see later,  $x$  is also used in specifying model parameters or retrieving state variables that are a function of position along a section (see **4.4 Range variables**).

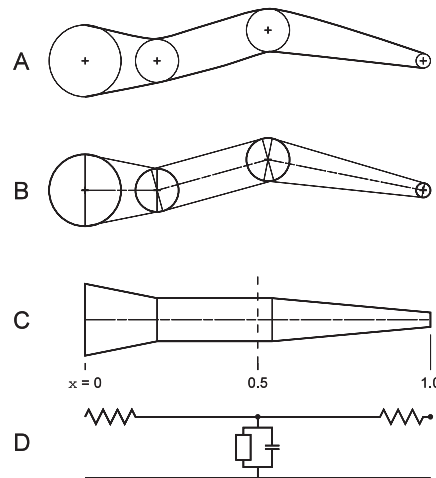


Figure 3.3. A: cartoon of an unbranched neurite (thick lines) that is to be represented by a section in a NEURON model. Computer-assisted morphometry generates a file that stores successive measurements of diameter (thin circles) centered at  $x, y, z$  coordinates (thin crosses). B: each adjacent pair of diameter measurements (thick circles) becomes the parallel faces of a truncated cone or frustum, the height of which is the distance between the measurement locations. The outline of each frustum is shown with thin lines, and a thin centerline passes through the central axis of the chain of solids. C: the centerline has been straightened so the faces of adjacent frusta are flush with each other. The scale underneath the figure shows the distance along the midline of the section in terms of the normalized position parameter  $x$ . The vertical dashed line at  $x = 0.5$  divides the section into two halves of equal length. D: Electrical equivalent circuit of the section as represented by a single segment (`nseg = 1`). The open rectangle includes all mechanisms for ionic (non-capacitive) transmembrane currents.

The special importance of  $x$  and `nseg` lies in the fact that they free the user from having to keep track of the correspondence between segment number and position on the nerve. In early versions of NEURON, all nerve properties were stored in vector variables where the vector index was the segment number. Changing the number of segments was an error prone and laborious process that demanded a remapping of the relationship between the user's mental image of the biologically important features of the model, on the one hand, and the implementation of this model in a digital computer, on the other. The use of  $x$  and `nseg` insulates the user from the most inconvenient aspects of such low-level details.

When  $nseg = 1$  the entire section is lumped into a single compartment. This compartment has only one node, which is located midway along its length, i.e. at  $x = 0.5$  (Fig. 3.3C and D). The integral of the surface area over the entire length of the section ( $0 \leq x \leq 1$ ) is used to calculate the membrane properties associated with this node. The values of the axial resistors are determined by integrating the cytoplasmic resistivity along the paths from the ends of the section to its midpoint (dashed line in Fig. 3.3C). The left and right hand axial resistances of Fig. 3.3D are evaluated over the  $x$  intervals  $[0, 0.5]$  and  $[0.5, 1]$ , respectively.

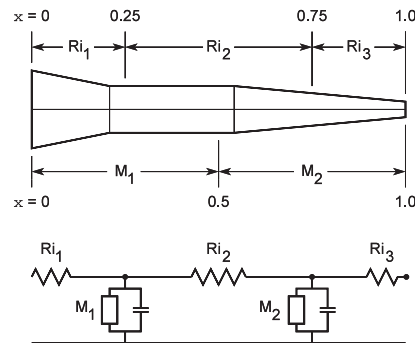


Figure 3.4. How the neurite of Fig. 3.3 would be represented by a section with two segments ( $nseg = 2$ ). Now the electrical equivalent circuit (bottom) has two nodes. The membrane properties attached to the first and second nodes are based on neurite dimensions and biophysical parameters over the  $x$  intervals  $[0, 0.5]$  and  $[0.5, 1]$ , respectively. The three axial resistances are computed from the cytoplasmic resistivity and neurite dimensions over the  $x$  intervals  $[0, 0.25]$ ,  $[0.25, 0.75]$ , and  $[0.75, 1]$ .

Fig. 3.4 shows what happens when  $nseg = 2$ . Now NEURON breaks the section into two segments of equal length that correspond to  $x$  intervals  $[0, 0.5]$  and  $[0.5, 1]$ . The membrane properties over these intervals are attached to the nodes at 0.25 and 0.75, respectively. The three axial resistors  $Ri_1$ ,  $Ri_2$  and  $Ri_3$  are determined by integrating the path resistance over the  $x$  intervals  $[0, 0.25]$ ,  $[0.25, 0.75]$ , and  $[0.75, 1]$ .

### 3.3 Integration methods

Spatial discretization reduced the cable equation, a partial differential equation with derivatives in space and time, to a set of ordinary differential equations with first order derivatives in time. Selection of an integration method to solve these equations is guided by concerns of stability, accuracy, and efficiency (Hines and Carnevale 1995).

NEURON offers the user a choice of two stable implicit integration methods: backward Euler, and a variant of Crank-Nicholson (C-N). Backward Euler is the default because of its robust numerical stability properties. Backward Euler can be used with extremely large time steps in order to find the steady-state solution for a linear (“passive”) system. It produces good qualitative results even with large time steps, and it works even if some or all of the equations are strictly algebraic relations among states.

A method which is more accurate for small time steps is available by setting the global parameter `secondorder` to 2. NEURON then uses a variant of the C-N method, in which numerical error is proportional to  $\Delta t^2$ .

Both of these are implicit integration methods, in which all current balance equations must be solved simultaneously. The backward Euler algorithm does not resort to iteration to deal with nonlinearities, since its numerical error is proportional to  $\Delta t$  anyway. The special feature of the C-N variant is its use of a

staggered time step algorithm to avoid iteration of nonlinear equations (see **3.3.1 Efficiency** below). This converts the current balance part of the problem to one that requires only the solution of simultaneous *linear* equations.

Although the C-N method is formally stable, it is sometimes plagued by spurious large amplitude oscillations (see Fig. 7 in Hines and Carnevale (1995)). This occurs when  $\Delta t$  is too large, as may occur in models that involve fast voltage clamps or that have compartments which are coupled by very small resistances. However, C-N is safe in most situations, and it can be much more efficient than backward Euler for a given accuracy.

These two methods are almost identical in terms of computational cost per time step (see **3.3.1 Efficiency** below). Since the current balance equations have the structure of a tree (there are no current loops), direct gaussian elimination is optimal for their solution (Hines 1984). This takes exactly the same number of computer operations as would be required for an unbranched cable with the same number of compartments.

For any particular problem, the best way to determine which is the method of choice is to compare both methods with several values of  $\Delta t$  to see which allows the largest  $\Delta t$  consistent with the desired accuracy. In performing such trials, one must remember that the stability properties of a simulation depend on the *entire* system that is being modeled. Because of interactions between the “biological” components and any “nonbiological” elements, such as stimulators or voltage-clamps, the time constants of the entire system may be different from those of the biological components alone. A current source (perfect current clamp) does not affect stability because it does not change the time constants. Any other signal source imposes a load on the compartment to which it is attached, changing the time constants and potentially requiring use of a smaller time step to avoid numerical oscillations in the C-N method. The more closely a signal source approximates a voltage source (perfect voltage clamp), the greater this effect will be.

### 3.3.1 Efficiency

Nonlinear equations generally need to be solved iteratively to maintain second order correctness. However, voltage dependent membrane properties, which are typically formulated in analogy to Hodgkin-Huxley (HH) type channels, allow the cable equation to be cast in a linear form, still second order correct, that can be solved without iterations. A direct solution of the voltage equations at each time step  $t \rightarrow t + \Delta t$  using the linearized membrane current  $I(V,t) = G \cdot (V - E)$  is sufficient as long as the slope conductance  $G$  and the effective reversal potential  $E$  are known to second order at time  $t + 0.5 \Delta t$ . HH type channels are easy to solve at  $t + 0.5 \Delta t$  since the conductance is a function of state variables which can be computed using a separate time step that is offset by  $0.5 \Delta t$  with respect to the voltage equation time step. That is, to integrate a state from  $t - 0.5 \Delta t$  to  $t + 0.5 \Delta t$  we only require a second order correct value for the voltage dependent rates at the midpoint time  $t$ .

Figure 3.5 contrasts this approach with the common technique of replacing nonlinear coefficients by their values at the beginning of a time step. For HH equations in a single compartment, the staggered time grid approach converts four simultaneous nonlinear equations at each time step to four independent linear equations that have the same order of accuracy at each time step. Since the voltage dependent rates use the voltage at the midpoint of the integration step, integration of channel states can be done analytically in just a single addition and multiplication operation and two table lookup operations. While this efficient scheme achieves second order accuracy, the tradeoff is that the tables depend on the value of the time step and must be recomputed whenever the time step changes.

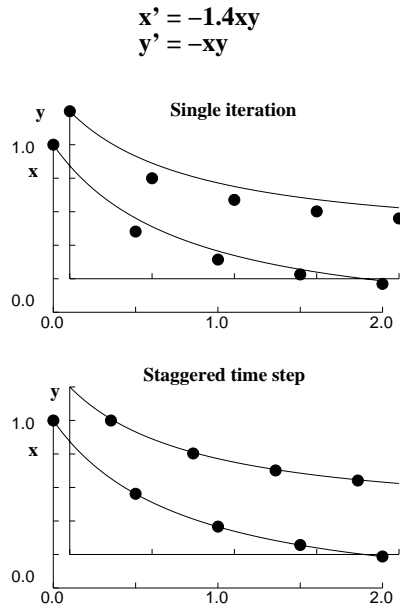


Figure 3.5. The equations shown at the top of the figure are computed using the Crank-Nicholson method. Top:  $x(t + \Delta t)$  and  $y(t + \Delta t)$  are determined using their values at time  $t$ . Bottom: staggered time steps yield decoupled linear equations.  $y(t + \Delta t/2)$  is determined using  $x(t)$ , after which  $x(t + \Delta t)$  is determined using  $y(t + \Delta t/2)$ .

Neuronal architecture can also be exploited to increase computational efficiency. Since neurons generally have a branched tree structure with no loops, the number of arithmetic operations required to solve the cable equation by Gaussian elimination is exactly the same as for an unbranched cable with the same number of compartments. That is, we need only  $O(N)$  arithmetic operations for the equations that describe  $N$  compartments connected in the form of a tree, even though standard Gaussian elimination generally takes  $O(N^3)$  operations to solve  $N$  equations in  $N$  unknowns. The tremendous efficiency increase results from the fact that, in a tree, one can always find a leaf compartment  $i$  that is connected to only one other compartment  $j$ , so that:

- 1) the equation for compartment  $i$  (Eq. 3a) involves only the voltages in compartments  $i$  and  $j$ , and
- 2) the voltage in leaf compartment  $i$  is involved only in the equations for compartments  $i$  and  $j$  (Eq. 3a and b).

$$a_{ii}V_i + a_{ij}V_j = b_i \quad (3a)$$

$$a_{ji}V_i + a_{jj}V_j + [\text{terms from other compartments}] = b_j \quad (3b)$$

Using Eq. 3a to eliminate the  $V_i$  term from Eq. 3b, which requires  $O(1)$  (instead of  $N$ ) operations, gives Eq. 4 and leaves  $N-1$  equations in  $N-1$  unknowns.

$$a'_{jj}V_j + [\text{terms from other compartments}] = b'_j \quad (4)$$

$$\text{where } a'_{jj} = a_{jj} - (a_{ij}a_{ji}/a_{ii}) \text{ and } b'_j = b_j - (b_i a_{ji}/a_{ii})$$

This strategy can be applied until there is only one equation in one unknown.

Assume that we know the solution to these  $N-1$  equations, and in particular that we know  $V_j$ . Then we can find  $V_i$  from Eq. 3a with  $O(1)$  step. Therefore the effort to solve these  $N$  equations is  $O(1)$  plus the effort needed to solve  $N-1$  equations. The number of operations required is independent of the branching structure, so a tree of  $N$  compartments uses exactly the same number of arithmetic operations as a one-dimensional cable of  $N$  compartments.

Efficient Gaussian elimination requires an ordering that can be found by a simple algorithm: choose the equation with the current minimum number of terms as the equation to use in the elimination step. This minimum degree ordering algorithm is commonly employed in standard sparse matrix solver packages. For example, NEURON's "Matrix" class uses the matrix library written by Stewart and Leyk (1994). This and many other sparse matrix packages are freely available on the Internet at <http://www.netlib.org>.

## 4. THE NEURON SIMULATION ENVIRONMENT

No matter how powerful and robust its computational engine may be, the real utility of any software tool depends largely on its ease of use. Therefore a great deal of effort has been invested in the design of the simulation environment provided by NEURON. In this section we first briefly consider general aspects of the high-level language used for writing NEURON programs. Then we turn to an example of a model of a nerve cell to introduce specific aspects of the user environment, after which we cover these features more thoroughly.

### 4.1 The hoc interpreter

NEURON incorporates a programming language based on hoc, a floating point calculator with C-like syntax described by Kernighan and Pike (Kernighan and Pike 1984). This interpreter has been extended by the addition of object-oriented syntax (not including polymorphism or inheritance) that can be used to implement abstract data types and data encapsulation. Other extensions include functions that are specific to the domain of neural simulations, and functions that implement a graphical user interface (see below).

With hoc one can quickly write short programs that meet most problem-specific needs. The interpreter is used to execute simulations, customize the user interface, optimize parameters, analyze experimental data, calculate new variables such as impulse propagation velocity, etc..

NEURON simulations are not subject to the performance penalty often associated with interpreted (as opposed to compiled) languages because computationally intensive tasks are carried out by highly efficient precompiled code. Some of these tasks are related to integration of the cable equation and others are involved in the emulation of biological mechanisms that generate and regulate chemical and electrical signals.

NEURON provides a built-in implementation of the microemacs text editor. Since the choice of a programming editor is highly personal, NEURON will also accept hoc code in the form of straight ASCII files created with any other editor.

### 4.2 A specific example

In the following example we show how NEURON might be used to model the cell in the top of Fig. 4.1. Comments in the hoc code are preceded by double slashes (`//`), and code blocks are enclosed in curly brackets (`{ }`).

#### 4.2.1 First step: establish model topology

One very important feature of NEURON is that it allows the user to think about models in terms that are familiar to the neurophysiologist, keeping numerical issues (e.g. number of spatial segments) entirely separate from the specification of morphology and biophysical properties. As noted in a previous section (**3.2 Spatial discretization . . .**), this separation is achieved through the use of one-dimensional cable “sections” as the basic building block from which model cells are constructed. These sections can be connected together to form any kind of branched cable and endowed with properties which may vary with position along their length.

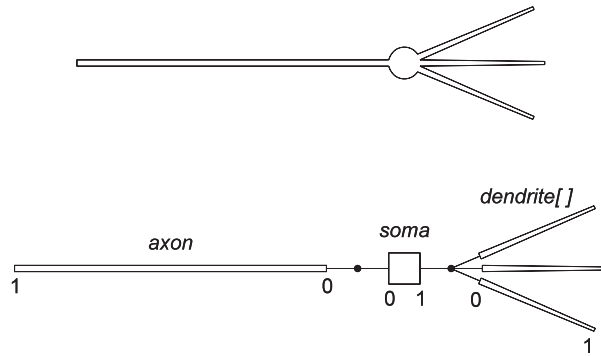


Figure 4.1. Top: cartoon of a neuron with a soma, three dendrites, and an unmyelinated axon (not to scale). The diameter of the spherical soma is  $50\ \mu\text{m}$ . Each dendrite is  $200\ \mu\text{m}$  long and tapers uniformly along its length from  $10\ \mu\text{m}$  diameter at its site of origin on the soma, to  $3\ \mu\text{m}$  at its distal end. The unmyelinated cylindrical axon is  $1000\ \mu\text{m}$  long and has a diameter of  $1\ \mu\text{m}$ . An electrode (not shown) is inserted into the soma for intracellular injection of a stimulating current. Bottom: topology of a NEURON model that represents this cell (see text for details).

The idealized neuron in Fig. 4.1 has several anatomical features whose existence and spatial relationships we want the model to include: a cell body (soma), three dendrites, and an unmyelinated axon. The following hoc code sets up the basic topology of the model:

```
create soma, axon, dendrite[3]
connect axon(0), soma(0)
for i=0,2 { connect dendrite[i](0), soma(1) }
```

The program starts by creating named sections that correspond to the important anatomical features of the cell. These sections are attached to each other using `connect` statements. As noted previously, each section has a normalized position parameter  $x$  which ranges from 0 at one end to 1 at the other. Because the axon and dendrites arise from opposite sides of the cell body, they are connected to the 0 and 1 ends of the `soma` section (see bottom of Fig. 4.1). A child section can be attached to any location on the parent, but attachment at locations other than 0 or 1 is generally employed only in special cases such as spines on dendrites.

### 4.2.2 Second step: assign anatomical and biophysical properties

Next we set the anatomical and biophysical properties of each section. Each section has its own segmentation, length, and diameter parameters, so it is necessary to indicate which section is being referenced. There are several ways to declare which is the currently accessed section, but here the most convenient is to precede blocks of statements with the appropriate section name.

```
// specify anatomical and biophysical properties
soma {
    nseg = 1           // compartmentalization parameter
    L = 50             // [μm] length
    diam = 50         // [μm] diameter
    insert hh         // standard Hodgkin-Huxley currents
    gnabar_hh = 0.5*0.120 // max HH sodium conductance
}
axon {
    nseg = 20
    L = 1000
    diam = 1
    insert hh
}
for i=0,2 dendrite[i] {
    nseg = 5
    L = 200
    diam(0:1) = 10:3 // dendritic diameter tapers along its length
    insert pas       // standard passive current
    e_pas = -65      // [mv] equilibrium potential for passive current
    g_pas = 0.001    // [siemens/cm2] conductance for passive current
}
```

The fineness of the spatial grid is determined by the compartmentalization parameter `nseg` (see **3.2 Spatial discretization . . .**). Here the soma is lumped into a single compartment (`nseg = 1`), while the axon and each of the dendrites are broken into several subcompartments (`nseg = 20` and `5`, respectively).

In this example, we specify the geometry of each section by assigning values directly to section length and diameter. This creates a “stylized model.” Alternatively, one can use the “3-D method,” in which NEURON computes section length and diameter from a list of (x, y, z, diam) measurements (see **4.5 Specifying geometry: stylized vs. 3-D**).

Since the axon is a cylinder, the corresponding section has a fixed diameter along its entire length. The spherical soma is represented by a cylinder with the same surface area as the sphere. The dimensions and electrical properties of the soma are such that its membrane will be nearly isopotential, so the cylinder approximation is not a significant source of error. If chemical signals such as intracellular ion concentrations were important in this model, it would be necessary to approximate not only the surface area but also the volume of the soma.

Unlike the axon, the dendrites become progressively narrower with distance from the soma. Furthermore, unlike the soma, they are too long to be lumped into a single compartment with constant diameter. The taper of the dendrites is accommodated by assigning a sequence of decreasing diameters to their segments. This is done through the use of “range variables,” which are discussed below (**4.4 Range variables**).

In this model the soma and axon contain Hodgkin-Huxley (HH) sodium, potassium, and leak channels (Hodgkin and Huxley 1952), while the dendrites have constant, linear (“passive”) ionic conductances. The

insert statement assigns the biophysical mechanisms that govern electrical signals in each section. Particular values are set for the density of sodium channels on the soma (`gnabar_hh`) and for the ionic conductance and equilibrium potential of the passive current in the dendrites (`g_pas` and `e_pas`). More information about membrane mechanisms is presented in a later section (**4.6 Density mechanisms and point processes**).

### 4.2.3 Third step: attach stimulating electrodes

This code emulates the use of an electrode to inject a stimulating current into the soma by placing a current pulse stimulus in the middle of the soma section. The stimulus starts at  $t = 1$  ms, lasts for 0.1 ms, and has an amplitude of 60 nA.

```
objref stim
soma stim = new IClamp(0.5) // put it in middle of soma
stim.del = 1 // [ms] delay
stim.dur = 0.1 // [ms] duration
stim.amp = 60 // [nA] amplitude
```

The stimulating electrode is an example of a point process. Point processes are discussed in more detail below (**4.6 Density mechanisms and point processes**).

### 4.2.4 Fourth step: control simulation time course

At this point all model parameters have been specified. All that remains is to define the simulation parameters, which govern the time course of the simulation, and write some code that executes the simulation.

This is generally done in two procedures. The first procedure initializes the membrane potential and the states of the inserted mechanisms (channel states, ionic concentrations, extracellular potential next to the membrane). The second procedure repeatedly calls the built-in single step integration function `fadvance()` and saves, plots, or computes functions of the desired output variables at each step. In this procedure it is possible to change the values of model parameters during a run.

```
dt = 0.05 // [ms] integration time step
tstop = 5 // [ms]
finitialize(-65) // initialize membrane potential, state variables, and time

proc integrate() {
  print t, soma.v(0.5) // show starting time
  // and initial somatic membrane potential
  while (t < tstop) {
    fadvance() // advance solution by dt
    // function calls to save or plot results would go here
    print t, soma.v(0.5) // show present time
    // and somatic membrane potential
    // statements that change model parameters would go here
  }
}
```

The built-in function `finitialize()` initializes time  $t$  to 0, membrane potential  $v$  to  $-65$  mV throughout the model, and the HH state variables  $m$ ,  $n$  and  $h$  to their steady state values at  $v = -65$  mV. Initialization can also be performed with a user-written routine if there are special requirements that `finitialize()` cannot accommodate, such as nonuniform membrane potential.

Both the integration time step  $dt$  and the solution time  $t$  are global variables. For this example  $dt = 50 \mu\text{s}$ . The `while()` statement repeatedly calls `fadvance()`, which integrates the model equations over the interval  $dt$  and increments  $t$  by  $dt$  on each call. For this example, the time and somatic membrane potential are displayed at each step. This loop exits when  $t \geq t_{\text{stop}}$ .

When this program is first processed by the NEURON interpreter, the model is set up and initiated but the `integrate()` procedure is not executed. When the user enters an `integrate()` statement in the NEURON interpreter window, the simulation advances for 5 ms using  $50 \mu\text{s}$  time steps.

### 4.3 Section variables

Three parameters apply to the section as a whole: cytoplasmic resistivity  $R_a$  ( $\Omega \text{ cm}$ ), the section length  $L$ , and the compartmentalization parameter  $n_{\text{seg}}$ . The first two are “ordinary” in the sense that they do not affect the structure of the equations that describe the model. Note that the hoc code specifies values for  $L$  but not for  $R_a$ . This is because each section in a model is likely to have a different length, whereas the cytoplasm (and therefore  $R_a$ ) is usually assumed to be uniform throughout the cell. The default value of  $R_a$  is  $35.4 \Omega \text{ cm}$ , which is appropriate for invertebrate neurons. Like  $L$  it can be assigned a new value in any or all sections (e.g.  $\sim 200 \Omega \text{ cm}$  for mammalian neurons).

The user can change the compartmentalization parameter  $n_{\text{seg}}$  without having to modify any of the statements that set anatomical or biophysical properties. However, if parameters vary with position in a section, care must be taken to ensure that the model incorporates the spatial detail inherent in the parameter description.

### 4.4 Range variables

Like dendritic diameter in our example, most cellular properties are functions of the position parameter  $x$ . NEURON has special provisions for dealing with these properties, which are called “range variables.” Other examples of range variables include the membrane potential  $v$ , and ionic conductance parameters such as the maximum HH sodium conductance  $g_{\text{nabar\_hh}}$  (siemens /  $\text{cm}^2$ ).

Range variables enable the user to separate property specification from segment number. A range variable is assigned a value in one of two ways. The simplest and most common is as a constant. For example, the statement `axon.diam = 10` asserts that the diameter of the axon is uniform over its entire length.

The syntax for a property that changes along a length of a section is `rangevar(xmin:xmax) = e1:e2`. The four italicized symbols are expressions with  $e1$  and  $e2$  being the values of the property at  $x_{\text{min}}$  and  $x_{\text{max}}$ , respectively. The position expressions must meet the constraint  $0 \leq x_{\text{min}} \leq x_{\text{max}} \leq 1$ . Linear interpolation is used to assign the values of the property at the segment centers that lie in the position range  $[x_{\text{min}}, x_{\text{max}}]$ . In this manner a continuously varying property can be approximated by a piecewise linear function. If the range variable is diameter, neither  $e1$  nor  $e2$  should be 0, or corresponding axial resistance will be infinite.

In our model neuron, the simple dendritic taper is specified by `diam(0:1) = 10:3` and `nseg = 5`. This results in five segments that have centers at  $x = 0.1, 0.3, 0.5, 0.7$  and  $0.9$  and diameters of 9.3, 7.9, 6.5, 5.1 and 3.7, respectively.

The value of a range variable at the center of a segment can appear in any expression using the syntax `rangevar(x)` in which  $0 \leq x \leq 1$ . The value returned is the value at the center of the segment containing  $x$ , NOT the linear interpolation of the values stored at the centers of adjacent segments. If the parentheses are omitted, the position defaults to a value of 0.5 (middle of the section).

A special form of the `for` statement is available: `for (var) stmt`. For each value of the normalized position parameter  $x$  that defines the center of each segment in the selected section (along with positions 0 and 1), this statement assigns `var` that value and executes the `stmt`. This hoc code would print the membrane potential as a function of physical position (in  $\mu\text{m}$ ) along the axon:

```
axon for (x) print x*L, v(x)
```

## 4.5 Specifying geometry: stylized vs. 3-D

As noted above (**4.2.2 Second step . . .**), there are two ways to specify section geometry. Our example uses the stylized method, which simply assigns values to section length and diameter. This is most appropriate when cable length and diameter are authoritative and 3-D shape is irrelevant.

If the model is based on anatomical reconstruction data (quantitative morphometry), or if 3-D visualization is paramount, it is best to use the 3-D method. This approach keeps the anatomical data in a list of  $(x, y, z, \text{diam})$  “points.” The first point is associated with the end of the section that is connected to the parent (this is not necessarily the 0 end!) and the last point is associated with the opposite end. There must be at least two points per section, and they should be ordered in terms of monotonically increasing arc length. This **pt3d list**, which is the authoritative definition of the shape of the section, automatically determines the length and diameter of the section.

When the `pt3d` list is non-empty, the shape model used for a section is a sequence of frusta. The `pt3d` points define the locations and diameters of the ends of these frusta. The effective area, diameter, and resistance of each segment are computed from this sequence of points by trapezoidal integration along the segment length. This takes into account the extra area introduced by diameter changes; even degenerate cones of 0 length can be specified (i.e. two points with same coordinates but different diameters), which add area but not length to the section. No attempt is made to deal with the effects of centroid curvature on surface area. The number of 3-D points used to describe a shape has nothing to do with `nseg` and does not affect simulation speed.

## 4.6 Density mechanisms and point processes

The `insert` statement assigns biophysical mechanisms, which govern electrical and (if present) chemical signals, to a section. Many sources of electrical and chemical signals are distributed over the membrane of the cell. These **density mechanisms** are described in terms of current per unit area and conductance per unit area; examples include voltage-gated ion channels such as the HH currents.

However, density mechanisms are not the most appropriate representation of all signal sources. Synapses and electrodes are best described in terms of localized absolute current in nanoamperes and conductance in microsiemens. These are called **point processes**.

An object syntax is used to manage the creation, insertion, attributes, and destruction of point processes. For example, a current clamp (electrode for injecting a current) is created by declaring an object variable and assigning it a new instance of the IClamp object class (see **4.2.3 Third step: attach stimulating electrodes**). When a point process is no longer referenced by any object variable, the point process is removed from the section and destroyed. In our example, redeclaring `stim` with the statement `objref stim` would destroy the pulse stimulus, since no other object variable is referencing it.

The location of a point process can be changed with no effect on its other attributes. In our example the statement `dendrite[2] stim.loc(1)` would move the current stimulus to the distal end of the third dendrite.

Many user-defined density mechanisms and point processes can be simultaneously present in each compartment of a neuron. One important difference between density mechanisms and point processes is that any number of the same kind of point process can exist at the same location.

User-defined density mechanisms and point processes can be linked into NEURON using the model description language NMODL. This lets the user focus on specifying the equations for a channel or ionic process without regard to its interactions with other mechanisms. The NMODL translator then constructs the appropriate C program which is compiled and becomes available for use in NEURON. This program properly and efficiently computes the total current of each ionic species used, as well as the effect of that current on ionic concentration, reversal potential, and membrane potential. An extensive discussion of NMODL is beyond the scope of this article, but its major advantages can be listed succinctly.

1. Interface details to NEURON are handled automatically — and there are a great many such details.
  - NEURON needs to know that model states are range variables and which model parameters can be assigned values and evaluated from the interpreter.
  - Point Processes need to be accessible via the interpreter object syntax and density mechanisms need to be added to a section when the “insert” statement is executed.
  - If two or more channels use the same ion at the same place, the individual current contributions need to be added together to calculate a total ionic current.
2. Consistency of units is ensured.
3. Mechanisms described by kinetic schemes are written with a syntax in which the reactions are clearly apparent. The translator provides tremendous leverage by generating a large block of C code that calculates the analytic Jacobian and the state fluxes.
4. There is often a great increase in clarity since statements are at the model level instead of the C programming level and are independent of the numerical method. For example, sets of differential and nonlinear simultaneous equations are written using an expression syntax such as
 
$$\begin{aligned} x' &= f(x, y, t) \\ \sim g(x, y) &= h(x, y) \end{aligned}$$
 where the prime refers to the derivative with respect to time (multiple primes such as  $x''$  refer to higher derivatives) and the tilde introduces an algebraic equation. The algebraic portion of such systems of equations is solved by Newton’s method, and a variety of methods are available for solving the differential equations, such as Runge-Kutta or backward Euler.
5. Function tables can be generated automatically for efficient computation of complicated expressions.
6. Default initialization behavior of a channel can be specified.

## 4.7 Graphical interface

The user is not limited to operating within the traditional “code-based command-mode environment.” Among its many extensions to hoc, NEURON includes functions for implementing a fully graphical,

windowed interface. Through this interface, and without having to write any code at all, the user can effortlessly create and arrange displays of menus, parameter value editors, graphs of parameters and state variables, and views of the model neuron. Anatomical views, called “space plots,” can be explored, revealing what mechanisms and point processes are present and where they are located.

The purpose of NEURON’s graphical interface is to promote a match between what the user thinks is inside the computer, and what is actually there. These visualization enhancements are a major aid to maintaining conceptual control over the simulation because they provide immediate answers to questions about what is being represented in the computer.

The interface has no provision for constructing neuronal topology, a conscious design choice based on the strong likelihood that a graphical toolbox for building neuronal topologies would find little use. Small models with simple topology are so easily created in hoc that a graphical topology editor is unnecessary. More complex models are too cumbersome to deal with using a graphical editor. It is best to express the topological specifications of complex stereotyped models through algorithms, written in hoc, that generate the topology automatically. Biologically realistic models often involve hundreds or thousands of sections, whose dimensions and interconnections are contained in large data tables generated by hours of painstaking quantitative morphometry. These tables are commonly read by hoc procedures that in turn create and connect the required sections without operator intervention.

The basic features of the graphical interface and how to use it to monitor and control simulations are discussed elsewhere (Moore and Hines 1996). However, several sophisticated analysis and simulation tools that have special utility for nerve simulation are worthy of mention.

- The “Function Fitter” optimizes a parameterized mathematical expression to minimize the least squared difference between the expression and data.
- The “Run Fitter” allows one to optimize several parameters of a complete neuron model to experimental data. This is most useful in the context of voltage clamp data which is contaminated by incomplete space clamp or models that cannot be expressed in closed form, such as kinetic schemes for channel conductance.
- The “Electrotonic Workbench” plots small signal input and transfer impedance and voltage attenuation as functions of space and frequency (Carnevale et al. 1996). These plots include the neuromorphic (Carnevale et al. 1995) and L vs. x (O’Boyle et al. 1996) renderings of the electrotonic transformation (Brown et al. 1992; Tsai et al. 1994b; Zador et al. 1995). By revealing the effectiveness of signal transfer, the Workbench quickly provides insight into the “functional shape” of a neuron.

All interaction with these and other tools takes place in the graphical interface and no interpreter programming is needed to use them. However, they are constructed entirely within the interpreter and can be modified when special needs require.

## 4.8 Object-oriented syntax

### 4.8.1 Neurons

It is often convenient to deal with groups of sections that are related. Therefore NEURON provides a data class called a **SectionList** that can be used to identify subsets of sections. Section lists fit nicely with the “regular expression” method of selecting sections, used in earlier implementations of NEURON, in that

1. the section list is easily constructed by using regular expressions to add and delete sections
2. after the list is constructed it is available for reuse
3. it is much more efficient to loop over the sections in a section list than to pick out the sections accepted by a combination of regular expressions

This code

```
objref alldend
alldend = new SectionList()
forsec "dend" alldend.append()
forsec alldend print secname()
```

forms a list of all the sections whose names contain the string “dend” and then iterates over the list, printing the name of each section in it. For the example program presented in this report, this would generate the following output in the NEURON interpreter window

```
dendrite[0]
dendrite[1]
dendrite[2]
```

although in this very simple example it would clearly have been easy enough to loop over the array of dendrites directly, e.g.

```
for i = 0,2 {
    dendrite[i] print secname()
}
```

#### 4.8.2 Networks

To help the user manage very large simulations, the interpreter syntax has been extended to facilitate the construction of hierarchical objects. This is illustrated by the following code fragment, which specifies a pattern for a simple stylized neuron consisting of three dendrites connected to one end of a soma and an axon connected to the other end.

```
begintemplate Cell1
    public soma, dendrite, axon
    create soma, dendrite[3], axon
    proc init() {
        for i=0,2 connect dendrite[i](0), soma(0)
        connect axon(0), soma(1)
        axon insert hh
    }
endtemplate Cell1
```

Whenever a new instance of this pattern is created, the `init()` procedure automatically connects the soma, dendrite, and axon sections together. A complete pattern would also specify default membrane properties as well as the number of segments for each section.

Names that can be referenced outside the pattern are listed in the `public` statement. In this case, since `init` is not in the list, the user could not re-initialize by calling the `init()` procedure. Public names are referenced through a dot notation.

The particular benefit of using templates (“classes” in standard object oriented terminology) is the fact that they can be employed to create any number of instances of a pattern. For example,

```
objref cell[10][10]
for i=0,9 for j=0,9 cell[i][j]=new Cell1()
```

creates an array of 100 objects of type `Cell` that can be referenced individually via the object variable `cell`. In this example, `cell[4][5].axon.gnabar_hh(0.5)` is the value of the maximum HH sodium conductance in the middle of the axon of `cell[4][5]`.

As this example implies, templates offer a natural syntax for the creation of networks. However it is entirely up to the user to logically organize the templates in such a way that they appropriately reflect the structure of the problem. Generally, any given structural organization can be viewed as a hierarchy of container classes, such as cells, microcircuits, layers, or networks. The important issue is how much effort is required for the concrete network representation to support a range of logical views of the same abstract network. A logical view that organizes the cells differently may not be easy to compute if the network is built as an elaborate hierarchy. This kind of pressure tends to encourage relatively flat organizations that make it easier to implement functions that search for specific information. The bottom line is that network simulation design remains an ad hoc process that requires careful programming judgement.

One very important class of logical views that are not generally organizable as a hierarchy are those of synaptic organization. In connecting cells with synapses, one is often driven to deal with general graphs, which is to say, no structure at all.

In addition to the notions of classes and objects (a synapse is an object with a pre- and a postsynaptic logical connection) the interpreter offers one other fundamental language feature that can be useful in dealing with objects that are collections of other objects. This is the notion of “iterators,” taken from the Sather programming language (Murer et al. 1996). This is a separation of the process of iteration from that of “what is to be done for each item.” If a programmer implements one or more iterators in a collection class, the user of the class does not need to know how the class indexes its items. Instead the class will return each item in turn for execution in the context of the loop body. This allows the user to write

```
for layer1.synapses(syn, type) {
    // statements that manipulate the object reference named "syn"
    // (The iterator causes "syn" to refer, in turn,
    // to each synapse of a certain type in the layer1 object)
}
```

without being aware of the possibly complicated process of picking out these synapses from the layer (that is the responsibility of the author of the class of which `layer1` is an instance).

It is to be sadly emphasized that these kinds of language features, though very useful, do not impose any policy with regard to the design decisions users must make in building their networks. Different programmers express very different designs on the same language base, with the consequence that it is more often than not infeasible to reconcile slightly different representations of even very similar concepts.

An example of a useful way to deal uniformly with the issue of synaptic connectivity is the policy implemented in NEURON by Lytton (1996). This implementation uses the normal NMODL methodology to define a synaptic conductance model and enclose it within a framework that manages network connectivity.

## 5. SUMMARY

The recent striking expansion in the use of simulation tools in the field of neuroscience has been encouraged by the rapid growth of quantitative observations that both stimulate and constrain the

formulation of new hypotheses of neuronal function, and enabled by the availability of ever-increasing computational power at low cost. These factors have motivated the design and implementation of NEURON, the goal of which is to provide a powerful and flexible environment for simulations of individual neurons and networks of neurons. NEURON has special features that accommodate the complex geometry and nonlinearities of biologically realistic models, without interfering with its ability to handle more speculative models that involve a high degree of abstraction.

As we note in this paper, one particularly advantageous feature is that the user can specify the physical properties of a cell without regard for the strictly computational concern of how many compartments are employed to represent each of the cable sections. In a future publication we will examine how the NMODL translator is used to define new membrane channels and calculate ionic concentration changes. Another will describe the Vector class. In addition to providing very efficient implementations of frequently needed operations on lists of numbers, the vector class offers a great deal of programming leverage, especially in the management of network models.

NEURON source code, executables, and documents are available at <http://neuron.duke.edu> and <http://www.neuron.yale.edu>, and by ftp from <ftp.neuron.yale.edu>.

## **ACKNOWLEDGMENTS**

We wish to thank John Moore, Zach Mainen, Bill Lytton, and the many other users of NEURON for their encouragement, helpful suggestions, and other contributions. This work was supported by NIH grant NS 11613 (“Computer Methods for Physiological Problems”) to MLH and by the Yale Neuroengineering and Neuroscience Center (NNC).

## REFERENCES

- Bernander, O., Douglas, R.J., Martin, K.A.C., and Koch, C. Synaptic background activity influences spatiotemporal integration in single pyramidal cells. *Proc. Nat. Acad. Sci.* 88:11569-11573, 1991.
- Brown, T.H., Zador, A.M., Mainen, Z.F., and Claiborne, B.J. Hebbian computations in hippocampal dendrites and spines. In: *Single Neuron Computation*, edited by T. McKenna, J. Davis, and S.F. Zornetzer. San Diego: Academic Press, 1992, p. 81-116.
- Carnevale, N.T. and Rosenthal, S. Kinetics of diffusion in a spherical cell: I. No solute buffering. *J. Neurosci. Meth.* 41:205-216, 1992.
- Carnevale, N.T., Tsai, K.Y., Claiborne, B.J., and Brown, T.H. The electrotonic transformation: a tool for relating neuronal form to function. In: *Advances in Neural Information Processing Systems*, vol. 7, edited by G. Tesauro, D.S. Touretzky, and T.K. Leen. Cambridge, MA: MIT Press, 1995, p. 69-76.
- Carnevale, N.T., Tsai, K.Y., and Hines, M.L. The Electrotonic Workbench. *Society for Neuroscience Abstracts* 22:1741, 1996.
- Cauller, L.J. and Connors, B.W. Functions of very distal dendrites: experimental and computational studies of layer I synapses on neocortical pyramidal cells. In: *Single Neuron Computation*, edited by T. McKenna, J. Davis, and S.F. Zornetzer. San Diego: Academic Press, 1992, p. 199-229.
- Destexhe, A., Babloyantz, A., and Sejnowski, T.J. Ionic mechanisms for intrinsic slow oscillations in thalamic relay neurons. *Biophys. J.* 65:1538-1552, 1993a.
- Destexhe, A., Contreras, D., Sejnowski, T.J., and Steriade, M. A model of spindle rhythmicity in the isolated thalamic reticular nucleus. *J. Neurophysiol.* 72:803-818, 1994.
- Destexhe, A., Contreras, D., Steriade, M., Sejnowski, T.J., and Huguenard, J.R. In vivo, in vitro and computational analysis of dendritic calcium currents in thalamic reticular neurons. *J. Neurosci.* 16:169-185, 1996.
- Destexhe, A., McCormick, D.A., and Sejnowski, T.J. A model for 8-10 Hz spindling in interconnected thalamic relay and reticularis neurons. *Biophys. J.* 65:2474-2478, 1993b.
- Destexhe, A. and Sejnowski, T.J. G-protein activation kinetics and spill-over of GABA may account for differences between inhibitory responses in the hippocampus and thalamus. *Proc. Nat. Acad. Sci.* 92:9515-9519, 1995.
- Häusser, M., Stuart, G., Racca, C., and Sakmann, B. Axonal initiation and active dendritic propagation of action potentials in substantia nigra neurons. *Neuron* 15:637-647, 1995.
- Hines, M. Efficient computation of branched nerve equations. *Int. J. Bio-Med. Comput.* 15:69-76, 1984.
- Hines, M. A program for simulation of nerve equations with branching geometries. *Int. J. Bio-Med. Comput.* 24:55-68, 1989.
- Hines, M. NEURON—a program for simulation of nerve equations. In: *Neural Systems: Analysis and Modeling*, edited by F. Eeckman. Norwell, MA: Kluwer, 1993, p. 127-136.
- Hines, M. The NEURON simulation program. In: *Neural Network Simulation Environments*, edited by J. Skrzypek. Norwell, MA: Kluwer, 1994, p. 147-163.
- Hines, M. and Carnevale, N.T. Computer modeling methods for neurons. In: *The Handbook of Brain Theory and Neural Networks*, edited by M.A. Arbib. Cambridge, MA: MIT Press, 1995, p. 226-230.
- Hines, M. and Shrager, P. A computational test of the requirements for conduction in demyelinated axons. *J. Restor. Neurol. Neurosci.* 3:81-93, 1991.
- Hodgkin, A.L. and Huxley, A.F. A quantitative description of membrane current and its application to conduction and excitation in nerve. *J. Physiol.* 117:500-544, 1952.

- Hsu, H., Huang, E., Yang, X.-C., Karschin, A., Labarca, C., Figl, A., Ho, B., Davidson, N., and Lester, H.A. Slow and incomplete inactivations of voltage-gated channels dominate encoding in synthetic neurons. *Biophys. J.* 65:1196-1206, 1993.
- Jaffe, D.B., Ross, W.N., Lisman, J.E., Miyakawa, H., Lasser-Ross, N., and Johnston, D. A model of dendritic Ca<sup>2+</sup> accumulation in hippocampal pyramidal neurons based on fluorescence imaging experiments. *J. Neurophysiol.* 71:1065-1077, 1994.
- Kernighan, B.W. and Pike, R. Appendix 2: Hoc manual. In: *The UNIX Programming Environment*. Englewood Cliffs, NJ: Prentice-Hall, 1984, p. 329-333.
- Lindgren, C.A. and Moore, J.W. Identification of ionic currents at presynaptic nerve endings of the lizard. *J. Physiol.* 414:210-222, 1989.
- Lytton, W.W. Optimizing synaptic conductance calculation for network simulations. *Neural Computation* 8:501-509, 1996.
- Lytton, W.W., Destexhe, A., and Sejnowski, T.J. Control of slow oscillations in the thalamocortical neuron: a computer model. *Neurosci.* 70:673-684, 1996.
- Lytton, W.W. and Sejnowski, T.J. Computer model of ethosuximide's effect on a thalamic neuron. *Ann. Neurol.* 32:131-139, 1992.
- Mainen, Z.F., Joerges, J., Huguenard, J., and Sejnowski, T.J. A model of spike initiation in neocortical pyramidal neurons. *Neuron* 15:1427-1439, 1995.
- Mainen, Z.F. and Sejnowski, T.J. Reliability of spike timing in neocortical neurons. *Science* 268:1503-1506, 1995.
- Mascagni, M.V. Numerical methods for neuronal modeling. In: *Methods in Neuronal Modeling*, edited by C. Koch and I. Segev. Cambridge, MA: MIT Press, 1989, p. 439-484.
- Moore, J.W. and Hines, M. Simulations with NEURON 3.1, on-line documentation in html format, available at <http://neuron.duke.edu>, 1996.
- Murer, S., Omohundro, S.M., Stoutamire, D., and Szyerski, C. Iteration abstraction in Sather. *ACM Transactions on Programming Languages and Systems* 18:1-15, 1996.
- O'Boyle, M.P., Carnevale, N.T., Claiborne, B.J., and Brown, T.H. A new graphical approach for visualizing the relationship between anatomical and electrotonic structure. In: *Computational Neuroscience: Trends in Research 1995*, edited by J.M. Bower. San Diego: Academic Press, 1996.
- Rall, W. Theoretical significance of dendritic tree for input-output relation. In: *Neural Theory and Modeling*, edited by R.F. Reiss. Stanford: Stanford University Press, 1964, p. 73-97.
- Rall, W. Cable theory for dendritic neurons. In: *Methods in Neuronal Modeling*, edited by C. Koch and I. Segev. Cambridge, MA: MIT Press, 1989, p. 8-62.
- Softky, W. Sub-millisecond coincidence detection in active dendritic trees. *Neurosci.* 58:13-41, 1994.
- Stewart, D. and Leyk, Z. *Meschach: Matrix Computations in C*. Proceedings of the Centre for Mathematics and its Applications. Vol. 32. Canberra, Australia: School of Mathematical Sciences, Australian National University, 1994.
- Traynelis, S.F., Silver, R.A., and Cull-Candy, S.G. Estimated conductance of glutamate receptor channels activated during epscs at the cerebellar mossy fiber-granule cell synapse. *Neuron* 11:279-289, 1993.
- Tsai, K.Y., Carnevale, N.T., and Brown, T.H. Hebbian learning is jointly controlled by electrotonic and input structure. *Network* 5:1-19, 1994a.
- Tsai, K.Y., Carnevale, N.T., Claiborne, B.J., and Brown, T.H. Efficient mapping from neuroanatomical to electrotonic space. *Network* 5:21-46, 1994b.
- Zador, A.M., Agmon-Snir, H., and Segev, I. The morphoelectrotonic transform: a graphical approach to dendritic function. *J. Neurosci.* 15:1669-1682, 1995.